REMOiso forcing for the iPILPS Phase 1 Experiments and the performance of REMOiso in three domains

M. J. Fischer[1] and K. Sturm[1]

[1]ANSTO, Institute for Nuclear Geophysiology, Menai, 2234, Australia

<u>Address for correspondence</u>
Dr M. J. Fischer
Australian Nuclear Science and Technology Organisation
Lucas Heights Science and Technology Centre
Private Mail Bag 1
Menai
NSW 2234
Australia
Email mjf@ansto.gov.au

Abstract

Land surface schemes (and their evaluation) require high-quality forcing at subdiurnal resolution. The paucity of such data for land surface scheme experiments is exacerbated in iPILPS (Isotopes in the Project for Intercomparison of Land-surface Parameterisation Schemes), where high-quality, high-resolution **isotope** forcing is also required. The REgional MOdel REMOiso has been used to provide meteorological and isotopic forcing for several years for three sites for the iPILPS Phase 1 experiment: Manaus (Brazil), Neuherberg (near Munich, Germany) and Tumbarumba (Australia). Thus, this paper is about how the forcing data for the iPILPS Phase 1 experiment was generated, and how the model-derived forcing compares with observational data. The comparison between monthly aggregations of the REMOiso simulations and observational data such as GNIP (Global Network of Isotopes in Precipitation) shows that REMOiso produces plausible results for these three regions and sites. An extended example of the strength and weaknesses of REMOiso is shown, by presenting the first application of REMOiso to the Australian domain. These simulations are compared with temperature, precipitation and isotopic data, collected by GNIP and the Australian Bureau of Meteorology, for seven stations in Australia. Observational sampling campaigns will provide meteorological and isotopic data to compare how REMOiso performs at sub-diurnal resolution. The current forcing from REMOiso, however, provides a set of high resolution data, physically consistent with each other, that can be additionally used by modellers wishing to test the performance of their own isotope-enabled land surface schemes.

Keywords: water isotopes, regional climate model, REMOiso

1. Introduction

Quantitative scientific models of the world are mathematical functions that relate inputs (x) to outputs (y), y = *f*(x), where both x and y can be multi-vector matrices. In land surface modelling (LSM) experiments (e.g. the PILPS experiments, e.g. Chen *et al*. 1997), such functions are iterated through time for some spatio-temporal scale of a land-surface system. There are two possible sources of inputs for these experiments: i) observational data (in which case we would expect the LSM outputs to approximate observational outputs collected over the same spatiotemporal scale, if such a thing is possible) or ii) hypothetical forcing (which may - or may not - approximate reality). Both types of forcing are useful in model intercomparison experiments. Hypothetical forcing is especially useful when only patchy observational data exists. If the hypothetical forcing approximates reality, then experiments with ii) can also be useful as a preliminary step towards understanding and preparing for modelling experiments with i).

The iPILPS Phase 1 experiment (http://ipilps.ansto.gov.au/), which aims to compare how differently isotopically-enabled Land Surface Schemes (ILSSs) simulate the diurnal cycle of isotopic fluxes, requires forcing that contains isotopes in precipitation and atmospheric vapour at high (sub-diurnal) resolution (see Ngo-Duc *et al*. 2005 for a recent review on forcing sets for LSM experiments). For iPILPS, few such observational datasets with similar resolution are available; that is, isotopes in vapour and precipitation are not being measured continuously at fine timescales (currently, the highest resolution continuous studies at continental scale involve weekly sampling of precipitation only e.g. Welker 2000). Recent developments in the field of FTIR and TDL (i.e. the Fourier Transform Infra-red spectrometer: Griffith *et al.*, 2006, and the

Tunable Diode Laser spectrometer: Bowling *et al*., 2003) have led to the development of instruments that allow field sampling at high temporal resolution, and these are currently being employed to generate high-resolution observational isotope data for the iPILPS experiment. However, it will still be some time before this instrumental data is suitable to be used in a modelling experiment. In the absence of a comprehensive observational data set extending over at least four years at a 15 minute time resolution, we have to rely on an hypothetical forcing data set. Thus, iPILPS Phase 1 is a model intercomparison experiment which uses hypothetical forcing, as a step towards model intercomparison with observational forcing data. Instead of making up the forcing fields e.g. using spline functions of diurnal patterns, we believe that producing them by a climate model has following advantages: i) a wide range of 'diurnal scenarios' is covered, including seasonal and day-to-day variability, ii) the forcing variables, e.g. radiation, temperature and evaporation, are coherent with each other (to the extent permitted by REMOiso's physical parameterisations). Hence, if we are to learn from the Phase 1 experiments in this step, we need to establish the plausibility of the iPILPS Phase 1 forcing data.

2. Description of REMOiso model

The Regional Climate Model (RCM) REMO 5.0 (REgional MOdel) is a modified version of the numerical weather forecast model system EM/DM from the German Weather Service (Majewski 1991; Jacob 2001). REMO is a numerical three-dimensional regional climate model (RCM). Primitive equations, i.e. partial differential equations expressing the conservation of energy, vorticity assuming hydrostatical equilibrium and water content are numerically resolved at each integration time-step of the model. Processes that can't be explicitly resolved because their spatial or temporal characteristic size is below the model's resolution need to be parameterised. This applies e.g. for cloud micro-physics or turbulent fluxes through the boundary layer. In its current layout, REMO uses the same physical parameterisation scheme as the global circulation model (GCM) ECHAM v. 4 (Roeckner *et al.*, 1996). Horizontal discretisation is performed onto a rotated Arakawa-C grid, as a resolution of 0.5 degree (~53 km). At a later stage, the stable water isotopologues $H_2^{18}O$ and HDO were incorporated in REMO 5.0, as described in Sturm (2005a). The isotopic species undergo the same processes as the bulk water throughout the model. Whenever water phase changes occur, fractionation (both at equilibrium and under kinetical conditions) of the water isotopologues is computed. The physical equations governing isotopic fractionation during water phase change follow the isotope parameterisation established in ECHAMiso (Hoffmann *et al.* 1998, Werner and Heimann 2002). The isotopic parameterisation basically consists of a set of reservoirs (e.g. ocean, atmospheric vapour at different levels, soil water, surface water, leaf water etc), containing the most common water isotopologues. Moisture input is mixed unfractionated into any reservoir, but is generally fractionated when moisture leaves a reservoir by evaporation or condensation (whichever is appropriate). The two most important equations are:

$$(R_{reservoir})_t = (R_{reservoir})_{t-1} f^{(\alpha-1)} \qquad (1)$$

$$\alpha = R_{(evaporate\ or\ condensate)} / R_{reservoir} \qquad (2)$$

where,

$R_{reservoir}$ can be any reservoir (eg. ocean, cloud), note that $R_{reservoir} = ({}^{18}O:{}^{16}O)_{reservoir}$, or, $R_{reservoir} = ({}^{2}H:{}^{1}H)_{reservoir}$

It is important that α be appropriately adjusted (i.e. α or $1/\alpha$) for whether the situation is evaporation or condensation. Equations (1) and (2) are the Rayleigh isotopic distillation equations.

Additional major features of the isotope module are:

1) the isotopic tracers $H_2^{18}O$ and $HD^{16}O$ are treated as prognostic variables both for their liquid and gaseous phase;

2) evaporation from the sea-surface includes both equilibrium and wind-drift dependent kinetic fractionation [Merlivat and Jouzel, 1979];

3) the land surface module includes three prognostic reservoirs for isotopic tracers: (bucket) soil moisture, canopy interception and snow pack;

4) no discrimination is made between evaporation and transpiration from the soil moisture,

5) three-phase equilibrium and kinetic effects are accounted for in the fractionation processes in convective and stratiform clouds;

6) partial re-evaporation of rain drops below the cloud induces an isotopic re-equilibration with the surrounding moisture, at a rate of 45% for convective rainfall and 95% for large-scale rainfall. A more detailed description of REMOiso and its stable water isotope module can be found in Sturm (2005a).

The recently developed REMOiso, as the first operational isotope-enabled RCM, still relies on physical parameterisations optimised for coarser GCM. In particular, the parameterisation of hydrological processes at the surface are based on a 'bucket-type' representation of soil-moisture, which limits the resistance to evaporation and does not differentiate between the isotopic signature of transpiration versus evaporation. Furthermore, no specific parameterisation of the vegetation is present in REMOiso (apart from precipitation interception by the canopy). Hence we currently work on improving following parameterisations: the non-fractionating soil evaporation and transpiration, and the stomatal control of transpiration (see Braud *et al*. 2005 and Lai *et al*. 2005, who describe the complexities of water isotope fractionation in soil evaporation and plant transpiration), and the mesoscale convective parameterization and the fixed re-evaporation of rainfall below the cloud base (Schmidt *et al*. 2005 describe improve parameterisations of isotope cloud physics).

REMOiso was run over 3 domains, Europe, South America and Australia, to generate forcing data for four years for three sites for the iPILPS experiments: Neuherberg (48°N 11°E), Manaus (3°S 60°W) and Tumbarumba (35°S 148°E) respectively (but see below for caveats). The grid sizes for these domains were 81x91 cells, 161x101 cells and 101x91 cells, at 0.5° spatial resolution. In order to provide suitable forcing dataset for iPILPS, a routine was added to REMOiso to output forcing variables at the model integration time-step, for the selected iPILPS sites. The specifications of the three simulations by REMOiso are shown in Table 1. It is important to note that the order in which the runs from different domains were done does not matter, but the type of runs that were done for the individual domains does matter. A discussion of this for the three domains follows.

After one year spin-up, REMOiso was integrated over four years over the Australian domain, to produce five minute forcing data at Tumbarumba. These are the first runs of REMOiso over the Australian domain. Boundary conditions are provided by a climatological run by ECHAMiso at the T30 (3.75 degree) resolution. A climatological run is characterised by a permanent annual cycle in sea-surface temperatures (SST) and no constraints on the atmospheric circulation. In these runs, varying forcing data from one year to another should not be analysed as inter-annual variability, but rather as inherent variability of the atmospheric system.

The experimental set-up was similar for the simulation over the South American domain: REMOiso was nested in the same ECHAMiso T30 climatological simulation. Forcing data at Manaus was produced over one year using a high resolution output time-step of five minutes. This dataset is used for the EQY1 experiment in iPILPS. In the original runs of REMOiso over South America (performed prior to, and separate from, iPILPS) , the simulation output was saved at a timestep of six hours. This was not sufficient for the iPILPS experiments. Unfortunately, due to the time limitations imposed upon the iPILPS experiment by its creators, it was possible to re-run REMOiso over the entire South American domain for one year only. To generate additional data for the iPILPS experiment, a new statistical technique was developed to reconstruct similar five minute forcing data for three previously computed years, based on their six hour output. This new statistical technique, and its application to downscaling, will be documented in a future paper (it can be widely applied outside the iPILPS experiment), and is only briefly described here:

Take an autoregressive function:

$$Y_t = \rho(Y_{t-1}) + a(X_t) + \varepsilon_t \tag{3}$$

where,

$X_t =$ 6 hour data

$Y_t =$ 5 minute data

Here, X and Y are both functional data spaces, i.e. they are described by a set of orthonormal basis vectors which explain (in this case) the daily cycle.

The appropriate FAR model (Functional Autoregressive Model, equation) was estimated for individual months (rather than a single model for the whole year), to take into account seasonal variation in the functional relationships. The orthonormal basis vectors were estimated using principal components analysis (PCA) of the daily data. The model also accounts for the day-day correlation between meteorological variables. The autocorrelation parameters in the FAR model were estimated using the method outlined in Damon and Guillas (2005). Thus, while the original runs of REMOiso over South America focussed on the monthly timescale and are reported in Sturm 2005a, Sturm *et al*. 2005b, the additional runs peformed for the iPILPS experiment (that aimed to investigate monthly and sub-diurnal timescales) are reported here.

The boundary conditions for the four year simulation over Europe differ from the type of conditions used for South America and Australia. Here, REMOiso was nested in a nudged simulation by ECHAMiso at the T42 resolution. The nudging procedure consists of on-line constraints on the models circulation, so that it reproduces general circulation patterns as assimilated by the ERA15 re-analyses (http://www.ecmwf.int/research/era/ERA-15/index.html). Furthermore, REMOiso itself was nudged towards ERA15 upper-level circulation by applying a spectral nudging technique (von Storch *et al.*, 2000). The nudging required a smaller integration time-step of three minutes for the four year simulation over Europe.

The three or five minute simulations for the three stations were aggregated at a fifteen minute time-step, and made available to iPILPS participants (see http://ipilps.ansto.gov.au/). Here we briefly review the application of REMOiso in Europe and South America (Sturm 2005a, Sturm *et al*. 2005b, Sturm *et al*. 2005c), and document its performance over the Australian domain.

3. Model-Observational comparison

The forcing variables for the iPILPS experiments, obtained from REMOiso, can be found in Table 1 in Henderson-Sellers *et al*. (2006). There are at least two scales at which this forcing can be investigated: monthly and diurnal. Examples of variable maps produced by REMOiso are shown in Figures 1-3.

Monthly timescale

On a monthly timescale, the isotopic content of precipitation is controlled by environmental factors such as temperature, precipitation amount, altitude, continental rain-out and precipitation recycling. A thorough discussion of these factors can already be found e.g. in Dansgaard, 1964; Rozanski *et al*., 1993; and Hoffmann *et al.,* 2005.

In this section, the REMOiso simulations are compared to data collected by the IAEA GNIP (Global Network of Isotopes in Precipitation, IAEA and WMO, 2001) and GHCN (Global Historic Climate Network, Willmott *et al*., 2000), at monthly resolution. This comparison is shown in Figure 4. The 25, 50 and 75% percentiles of diurnal averages (using the 15 minute timestep) over all available days (e.g. 30 days x

4 years) are shown as thin dashed lines. For the variable δ^{18}O, the diurnal average is weighted:

$$\text{Diurnal } \delta^{18}\text{O} = \frac{\sum_{all\ j} \Pr_j \delta^{18} O_j}{\sum_{all\ j} \Pr_j} \tag{4}$$

where, j = model timesteps within one day, Pr = precipitation per timestep, δ^{18}O = δ^{18}O per timestep. The mean of the same diurnal averages is also shown as a heavy grey line (obviously, the mean and 50% percentile will be similar if the Probability Distribution Function (PDF) is symmetric and unimodal, but dissimilar if the PDF is skewed). In comparison, the data from two observational sets (GHCN and GNIP) is an average monthly value over all available years (GNIP = dashed black heavy line, GHCN = solid black heavy line). Thus the absolute values of the observations and REMOiso simulations are not necessarily directly comparable (due to the spatial and temporal differences in length and scale of averaging of different datasets), but we expect the relative annual cycles to be comparable. Thus, the comparison is informative (see below). Note that in the Tumbarumba figures, there are two GNIP lines (dashed heavy lines) which show the two closest GNIP stations (Adelaide and Melbourne), because Tumbarumba is not itself a GNIP station (Manaus and Munich are). Although isotope interpolation schemes exist (using on the GNIP data, see Bowen and Revenaugh 2003), these are almost certainly inappropriate in Australia, where all the GNIP stations are low altitude coastal stations (except Alice Springs, an inland station), and hence do not see the altitude and continental rain-out effects on isotopes.

South America

Precipitation and its isotopic content for Manaus, on a monthly timescale, are shown in Figure 4. Manaus exhibits typical climate features of the inner Tropics. The amplitude of the annual cycle for temperature (2 K) is significantly less than its diurnal amplitude (5 K), as seen on Figure 8. Precipitation displays a clear seasonality, with a doubly-peaked rainy season in December and April. This is consistent with the inter-tropical convergence zone (ITCZ) passing twice annually above this nearly equatorial location. The double peaked shape of precipitation is more strongly marked in REMOiso (as it is global circulation models, e.g. in Vuille *et al.*, 2003) than it is in observations. The isotopic composition of rainfall is here negatively correlated to the amount of precipitation, in accordance with the amount effect (Dansgaard 1964, Rozanski *et al.* 1993). Yet the different $\delta^{18}O$ response between the April and December precipitation maximum further underlie the integrative character of the signal: not only the amount of local precipitation, but rather the rain-out rate along the air mass trajectory controls the $\delta^{18}O$ signal. REMOiso captures qualitatively well the seasonality in both precipitation and $\delta^{18}O$. Yet the parameterisation of convective cloud micro-physics produces excessive rainfall during the rainy season (the rainfall is also more isotopically depleted in December than in April, but the GNIP observations show the opposite). The excessive precipitation in December is partially inherited from misfits by the host model ECHAMiso. The latter explains the discrepancy between the mean and the median monthly weighted $\delta^{18}O$ during the months of June and October. Excessive precipitation, with very depleted isotopic signature dominates the monthly mean, whereas the median does not deviate as much from the GNIP observations. The overall offset by $\delta^{18}O$ of +2 ‰ is due to the non-differentiation of evaporation and transpiration: as all surface fluxes in the model are considered non-fractionating, the isotopic effect of recycling by the vegetation is over-estimated. Further discussion of these patterns is found in Sturm 2005a; Sturm *et al*. 2005b.

Europe

Neuherberg (near Munich) displays a clear seasonality for temperature, but a less pronounced one for precipitation in both the REMOiso simulations and the observational data (Figure 4). In this mid-latitude climate, temperature appears as being the main control on the $\delta^{18}O$ signal. REMOiso's physical scheme is optimised for the European domain, which explains the almost perfect (relative) match between model simulations and observational data for both temperature and precipitation. The modelled $\delta^{18}O$ is overestimated by 1 ‰ as compared to the GNIP observations, with the largest discrepancies occurring in spring and summer (March – August). The non-fractionating surface fluxes, which neglects the depletion of evaporative fluxes by assimilating it to relatively enriched transpiration fluxes, is the main factor responsible for the offset. Furthermore, the bias can be related to the high number of small precipitation events (usually less depleted) in the REMOiso weighted mean, which are not accounted for in the GNIP measurements. Further documentation of the application of REMOiso in the European domain, is found in Sturm 2005a; Sturm *et al*. 2005c.

Australia

Apart from Sturm 2005a (Appendix C), this is the first report of the performance of REMOiso in the Australian domain, so it is important to discuss the model-observational comparison for a wider range of stations (apart from the site of Tumbarumba used in the iPILPS experiments). Here, the REMOiso simulations are also compared with data from the Australian Bureau of Meteorology (ABOM), since this provides more reliable data for the Australian region (based on continuous 30+ year climatology). The GNIP dataset provides the only comparable isotope data. Temperature, rainfall, and $\delta^{18}O$ on a monthly timescale are shown in Figures 5-7. The boxplots show the probability distribution of REMOiso variables over the number of years of simulation, and also over the 9 grid squares closest to each station (i.e. n = 4 years x 9 cells for each month), while the red lines show the mean (or additionally, the mean daily minimum and maximum values for the case of temperature) over the 30+ year climatology from selected ABOM stations. For mean temperature, REMOiso approximates the mean of the observational minimum and maximum, except in Tasmania (Cape Grim) where REMOiso temperatures are too warm during the winter season. In the REMOiso simulation, Adelaide, Alice Springs and Brisbane all show relatively low amounts of monthly rainfall, and Darwin has a distinct wet and dry season (but the wet season is drier than observed). Cape Grim and Melbourne are too wet during the winter and Perth is too dry. The isotopic content of precipitation is shown in Figure 7. Some stations show similar both an observed and modelled seasonal cycle (Cape Grim, Melbourne), but others do not (Alice Springs). There may be several reasons for these anomalies. Firstly, there may be spatial scale issues. The rainfall schemes in REMOiso are the same as those in its parent model, ECHAMiso, and those rainfall schemes may not operate properly at higher temporal and spatial resolution (Molinari and Dudek 1991). This may explain the positive rainfall anomalies over the Southern Ocean (and Cape Grim and Melbourne). Alternatively, REMOiso may inherit misfits from its parent model, ECHAMiso (current problems in ECHAMiso and other isotope-enabled GCM's are discussed in Hoffmann *et al*. 2005). Secondly, REMOiso has an unusual land-sea contrast (e.g. this causes Perth to be too dry in the winter, when the surrounding ocean cells have high rainfall - see Figure 1c). Thirdly, the isotopic content of precipitation may be affected by computational errors associated with small amounts of precipitation. The seasonal amount effect in Darwin and Alice Springs is not strong because of a positive bias in the precipitation isotope ratio, associated with relatively small amounts of precipitation. These small amounts of rainfall are likely to be isotopically enriched (either due to less rainout or to the partial evaporation of precipitation). Further, in REMOiso the partial evaporation of precipitation in the undersaturated sub-cloud atmosphere is fixed at 45% and 95% for convective and stratiform precipitation respectively. There have been no observational studies in Australia to determine these parameters for Australian rainfall. Fourthly, the relatively low precipitation in northern Australia (e.g. Darwin and Alice Springs) may be due to the inability of REMOiso to properly simulate tropical cyclones (e.g. see Camargo *et al*. 2005) In northern Austrlia, tropical cyclones (and associated intense low pressure troughs) generate approximately 50% of annual rainfall (Linacre and Hobbs 1991).

Figure 4 focusses on the site of Tumbarumba (used in the iPILPS experiment). The heavy lines show the GHCN (solid) for Tumbarumba, and GNIP (dashed) lines for the 2 closest GNIP stations: Melbourne and Adelaide. The validity of the latter comparison with the REMOiso Tumbarumba simulations is questionable since these GNIP stations are low-altitude coastal stations (except Alice Springs), whereas Tumbarumba is an alpine, inland station (altitude is ~1200m). However, we show the comparison here as currently there are no other monthly (or higher resolution) rainfall isotope data available for Tumbarumba.. There are valid expectations here, though: the simulations of temperature and rainfall isotopes should exhibit a greater seasonality than the respective data for the coastal GNIP stations (due to altitudinal effects). REMOiso reproduces the temperature and rainfall seasonality in the GHCN data, although the wet-season rainfall peak is of smaller duration in REMOiso (July-September) than in GHCN (May-October). REMOiso also reproduces the seasonal cycle in $\delta^{18}O$, which, as expected, has a greater seasonality than the two nearest GNIP stations. Observational campaigns (e.g. Moisture Isotopes in the Biosphere and Atmosphere program, Twining *et al*. 2006) have been initiated to provide better observational rainfall isotope data for many stations globally, including Tumbarumba.

Diurnal timescale

Although observational data at six hour intervals can be obtained from datasets such as the NCEP Reanalysis (National Centres for Environmental Prediction, http://www.cdc.noaa.gov/cdc/reanalysis/reanalysis.shtml), this data is coarse compared to the REMOiso simulations, and does not properly show diurnal variation in variables such as precipitation and humidity, that may have diurnal patterns more complicated than a simple single 'cycle'. Further, the NCEP Reanalysis contains no isotope information (and GNIP is only at monthly resolution). Hence, the investigation of the diurnal patterns in REMOiso simulations, here, focusses on the relative patterns between different variables, rather than their absolute values. In comparison to the monthly patterns discussed above, the factors responsible for sub-diurnal scale variation in isotopes in precipitation and vapour are much less understood (e.g., are day-day changes in storm isotope values due primarily to the intensity, duration or number of storms in a day? This is currently being investigated by the authors and will be the topic of a future paper). Note, though, that some of the monthly effects mentioned above can be observed in the REMOiso simulations in Figures 9, 11 and 13. In these Figures, the isotopic composition of the atmospheric vapour is higher in the summer than winter for the mid-latitude stations of Munich and Tumbarumba, and vice versa for the low latitude station, Manaus. This is due to two main factors: the higher summer temperatures (which change the initial condensation temperature of an airmass), and the increase in transpiration (which recycles moisture, that is relatively enriched compared to atmospheric vapour, back into the atmosphere) (see Fricke and O'Neil 1999). The latter phenomenon is also responsible for the afternoon enrichment in isotopic vapour in Munich (transpiration is relatively enhanced in the winter after midday) (Figure 11). However, Manuas and Tumbarumba show no such daily pattern in the isotopic composition of vapour (Figures 9 and 13). This anomaly can only be resolved by further investigation of the hydrology/isotope parameterisation in REMOiso. The daily pattern for the three iPILPS stations is discussed in more detail below.

South America

Figures 8 and 9 show examples (January and July) of forcing variables obtained from REMOiso for Manaus (Figures 8-13 show classical boxplots based on monthly data for each hour of a day over the four years of simulation; hence the 24 (hour) medians show the "median diurnal pattern" for a particular month, etc.). It is important to remember here that, for Manaus, simulations are interpolated for years 2-4, based on functional relationships between the six hour and five minute time scales for year 1. All meteorological variables show simple diurnal patterns in both January and July, presumably due to the strong diurnal convective pattern found generally in equatorial sites. The isotopic variation in both rainfall and vapour are more difficult to interpret. In tropical rainfall, an expectation is that there should be an inverse correlation between rainfall isotopic content and storm intensity (Yapp 1982). However, a strong inverse correlation does not appear in Figure 9 (In July there is a slight inverse correlation in isotope ratio and amount hr^{-1} for the hours 11-16). The main reason for this seems to be that small values of rainfall are characterised by large isotopic depletion (e.g. the hours from 1-9 or 20-24 in Figure 9 are characterised by isotope ratios that are similar to the the hours with higher rainfall intensities). This points to 'small value problems' in the model or in the interpolation scheme, that is, that small values of moisture contain 'unobserved' isotope ratios (i.e. isotope values that are far more positive or negative than that observed in nature, because people do not generally measure isotope ratios of, say, 0.2 mm of rainfall). A plot of isotope ratio against amount for hourly values of rainfall show that below about 0.2 mm, the isotope ratios of rainfall can basically assume any value. This hides patterns that are known from observational studies. A study on the effect of isotopic distillation by individual storms on daily variation will appear in a future paper.

Europe

Figures 10 and 11 show examples (January and July) of forcing variables obtained from REMOiso for Neuherberg. In January, at Neuherberg, along with the regular diurnal cycles of surface air temperature and shortwave radiation (Down. SW), there is a midday-afternoon trough in downward longwave radiation (Down. LW) and peak in humidity (Qair). Precipitation (PREC) and its isotopic content (δPREC18) do not show a simple diurnal pattern. The isotopic content of the atmospheric vapor peaks in the afternoon, presumably due to diurnal mixing with transpiration (the soil water and transpiration are isotopically enriched relative to the atmospheric vapour, Gat 1996). The January precipitation isotopic content shows a slight diurnal pattern (e.g. there is a 'bimodal' increase in amount hr^{-1} after midday, associated with relative isotopic depletion in the median or lower quantile δ values.) This is likely to result from isotopic distillation. In July, downward longwave radiation increases in the afternoon, accompanied by a trough in humidity, and isotopic depletion of the vapour. The change is smaller than (and opposite to) the January diurnal vapour isotope change, perhaps because the transpiration effect is offset by warmer summer temperatures (and hence the summer vapour is relatively enriched). July precipitation occurs in the late afternoon, and the rainout over these hours is accompanied by isotopic depletion (the rainfall isotope boxplot whiskers for hours 16-18 are skewed towards more negative values).

Australia

Figures 12 and 13 show examples (January and July) of forcing variables obtained from REMOiso for Tumbarumba. In January, at Tumbarumba, the variables surface air temperature, U-wind and downward shortwave and longwave radiation are characterised by simple diurnal cycles (day-night), while air pressure and V-wind show morning-afternoon change. January rainfall tends to occur in the morning, associated with higher values of humidity, and relatively depleted rainfall isotope values, presumably due to isotopic rainout. Similar patterns in the micrometeorological variables are seen in July, except that there is greater variance especially in wind and air pressure (this variance is due to variance betweeen different years). The patterns between rainfall and isotopic content are also more complex, and rainfall peaks occur in both the morning and afternoon and are relatively small (especially the medians) as expected from the high pressure system that dominates the Australian continent during the winter season.

4. Conclusions

In order to produce forcing for the iPILPS Phase 1 experiments, REMOiso has been run at a high temporal and spatial resolution in three regions. iPILPS uses atmosphere to land fluxes from REMOiso to provide forcing data for off-line land surface experiments focussed on three stations: Tumbarumba, Manaus, and Neuherberg (Munich). Here it has been shown that the monthly aggregation of these high resolution simulations produces results that are comparable with observational climatologies of stations in three regions: South America, Europe and Australia. The average diurnal patterns show both spatial and seasonal differences, using the example of just three stations. Some anomalies have been noticed in REMOiso, which are due to several factors, including spatial scale issues, inherited errors, small value problems, observationally-unknown parameters, isotopically non-fractionating soil evaporation, and synoptic feature problems (e.g. tropical cyclones). Despite these anomalies, REMOiso produces a forcing dataset for the three stations that is physically consistent, and hence suitable to be used in land-surface modelling experiments. The ongoing collection of high-resolution observational data from the regions investigated will also help to assess how REMOiso performs at finer timescales (e.g. Griffith *et al.*, 2006). While, the discussion here has focussed on comparing REMOiso simulations with observational data at monthly and daily resolution, future comparisons will focus on the finer timescale, including the stochastic properties of sets of individual storms.

Acknowledgments

We are grateful to the iPILPS team that chose to use REMOiso in their experiments, and to the three anonymous reviewers whose comments have improved this paper.

References

Bowen G. J., and Revenaugh J., 2003. Interpolating the isotopic composition of modern meteoric precipitation. *Water Resources Research,* 39, 1299, doi:10.129/2003WR002086.

Bowling, D.R., Sargent, S. D., Tanner, B. D, and Ehleringer, J. R., 2003. Tunable diode laser absorption spectroscopy for stable isotope studies of ecosystem-atmosphere CO_2 exchange. *Agricultural and Forest Meteorology*, 118, 1-19.

Braud, I., Bariac, T., Gaudet, J. P. and Vauclin, M. 2005. SiSPAT-Isotope, a coupled heat, water and stable isotope (HDO and $H_2{}^{18}O$) transport model for bare soil. Part I. Model description and first verifications. *Journal of Hydrology*, 309, 277-300.

Camargo, S. J., Barnston, A. G. Zebiak, S. E., 2005. A statistical assessment of tropical cyclone activity in atmospheric general circulation models. *Tellus*, 57A, 589-604.

Chen T.H., Henderson-Sellers, A., Milly, P.C.D., Pitman, A.J., Beljaars, A.C.M., Polcher, J., Abramopoulos, F., Boone, A., Chang, S., Chen, F., Dai, Y., Desborough, C.E., Dickinson, R.E., Dumenil, L., Ek, M., Garratt, J.R., Gedney, N., Gusev, Y.M., Kim, J., Koster, R., Kowalczyk, E.A., Laval, K., Lean, J., Lettenmaier, D., Liang, X., Mahfouf, J.-F., Megelkamp, H.-T., Mitchell, K., Nasonova, O.N., Noilhan, J., Robock, A., Rozensweig, C., Schaake, J., Schlosser, A., Schulz, J.P., Shao, Y., Shmakin, A.B., Verseghy, D.L., Wetzel, P., Wood, E.F., Xue, Y., Yang, Z.-L. and Zeng, Q., 1997. Cabauw Experimental results from the project for Intercomparison of Land-surface Parameterization Schemes. *J. Climate,* 10**,** 1194-1215

Damon, J. and Guillas, S., 2005. Estimation and simulation of autoregressive Hilbertian processes with exogenous variables. *Statistical Inference for Stochastic processes*, 8, 185-204.

Dansgaard, W., 1964. Stable isotopes in precipitation. *Tellus*, XVI, 436 – 468.

Fricke, H. C. and O'Neil, J. R. 1999. The correlation between $^{18}O/^{16}O$ ratios of meteoric water and surface temperature: its use in investigating terrestrial climate change over geologic time. *Earth and Planetary Science*, 170, 181-196.

Griffith, D. W. T., Williams, A. G., Kettlewell, G. and Leuning, R., 2006. Partitioning evaporation and transpiration in a forest ecosystem by real time continuous field measurements of $\delta^{18}D$ in water vapour. *Global and Planetary Change*, submitted.

Henderson-Sellers, A., Fischer, M. J., Aleinov, I., McGuffie, K., Riley, W. J., Schmidt, G. A., Sturm1, K., Yoshimura, K and Irannejad, P. 2006. Stable water isotope simulation by current land-surface schemes: Results of iPILPS Phase 1. *Global and Planetary Change*, submitted.

Hoffmann, G., Werner, M., and Heimann, M., 1998. Water isotope module of the ECHAM atmospheric general circulation model: A study on timescales from days to several years. *Journal of Geophysical Research*, 103, 16871 – 16896.

Hoffmann, G., Cuntz, M., Werner, M., and Jouzel, J. 2005. A systematic comparison between the IAEA/GNIP isotope network and Atmospheric General Circulation Models: How much climate information is in the water isotopes? *Hydrological Processes,* submitted.

International Atomic Energy Agency IAEA and World Meteorological Organisation WMO, 2001. The Global Network of Isotopes in Precipitation (GNIP) database. "http://isohis.iaea.org" , 2001.

Jacob, D., 2001. A note to the simulation of the annual and inter-annual variability of the water budget over the Baltic Sea drainage basin. *Meteorology and Atmospheric Physics*, 77, 61 – 73.

Lai, C., Ehleringer, J. R., Bond, B. J. and Tha Paw U, K., 2005. Contributions of evaporation, isotopic non-steady state transpiration and atmospheric mixing on the $\delta^{18}O$ of water vapour in Pacific Northwest coniferous forests. *Plant, Cell and Environment*, in press.

Linacre, E. and Hobbs, J. E., 1991. *The Australian Climatic Environment*. John Wiley and Sons, Brisbane.

Majewski, D., 1991. The Europa-Modell of the DeutscherWetterdienst. *ECMWF Seminar on numerical methods in atmospheric models*, **2**, 147 – 191.

Merlivat, L. and Jouzel, J. 1979. Global climatic interpretation of the deuterium-oxygen 18 relationship for precipitation. *Journal of Geophysical Research*, 84, 5029 – 5033.

Molinari, J., Dudek, M. 1991. Parameterisation of convective precipitation in mesoscale numerical models: a crtical review. *Monthly Weather Review*, 120, 326-344.

Ngo-Duc, T., Polcher, J. and Laval, K., 2005. A 53-year forcing data set for land surface models. *Journal of Geophysical Research*, 110, D06116, doi:10.1029/2004JD005434.

Roeckner, E., Arpe, E. K., Bengtsson, L., Christoph, M., Claussen, M., Dümenil, L. Esch, M. Giorgetta, M. Schlese, U. and Schulzweida, U. 1996. The atmospheric circulation model ECHAM-4: model description and simulation of the present day climate. *Technical Report 218*. Max-Planck-Institute für Meteorologie, Germany.

Rozanski, K., Araguás-Araguás, L., and Gonfiantini, R., 1993. Isotopic patterns in modern global precipitation. In: Swart, P. K., Lohmann, K. C., MacKenzie, J. and Savin, S. (Eds.), *Climatic Change in Continental Isotope Records*. American Geophysical Union, Washington, pp. 1–37.

Schmidt, G. A., Hoffman, G., Shindell, D. T, Hu, Y., 2005. Modelling atmospheric stable water isotopes and the potential for constraining cloud processes and stratosphere-troposphere water exchange. *Journal of Geophysical Research*, submitted.

von Storch, H., Langenberg, H., and Feser, F., 2000. A spectral nudging technique for dynamical downscaling purposes. *Monthly Weather Review*, 128, 3664–3673.

Sturm, K., 2005a. Regional atmospheric modelling of the stable water isotope cycle. PhD Thesis, Université Joseph Fourier – Grenoble I, available at http://lgge.obs.ujf-grenoble.fr/publiscience/theses/these-sturm.pdf

Sturm, K., Hoffmann, G., and Langmann, B., 2005b. Climatology of stable water isotopes in South America: comparing general to regional circulation models. *Journal of Climate*, submitted.

Sturm, K., Hoffmann, G., Langmann, B. and Stichler, W., 2005c. Stable water isotopes in precipitation: a regional circulation modelling approach. *Hydrological Processes*, 19, 3425-3444, doi: 10.1002/hyp.5979.

Vuille, M., Bradley, R. S., Werner, M., Healy, R., and Keimig, F. 2003. Modeling $\delta^{18}O$ in precipitation over the tropical Americas: 1. Interannual variability and climatic controls. *Journal of Geophysical Research*, 108, D6, 4174, doi:10.1029/2001JD002038.

Welker J. M. 2000. Isotopic (^{18}O) characteristics of weekly precipitation collected across the USA: an initial analysis with application to water source studies. *Hydrological Processes*, 14,1449-1464.

Werner, M. and Heimann, M., 2002. Modeling interannual variability of water isotopes in Greenland and Antarctica. *Journal of Geophysical Research*, 107, 1-13, doi:10.1029/2001JD900253.

Willmott, C. J. and Matsuura, K., 2000. Terrestrial Air Temperature and Precipitation: Monthly and Annual Climatologies, version 3.01, Center for Climatic Research, University of Delaware, http://climate.geog.udel.edu/~climate/.

Yapp, C. J. 1982. A model for the relationships between precipitation D/H ratios and precipitation intensity. *Journal of Geophysical Research*, 87, 9614-9620.

Tables:

iPILPS site	***Boundary conditions***	***Time-step***	***Remarks***
Neuherberg	Nudged 1979 - 1982	3 minutes	4 years of data available
Manaus	Climatological	5 minutes	15 minute reconstructed forcing data for the first 3 years
Tumbarumba	Climatological	5 minutes	4 years of data available

Table 1: Technical specifications of the REMOiso simulations to provide iPILPS forcing datasets.

Figure captions:

Figure 1: REMOiso simulations of mean precipitation in mm month^{-1} (left panel) and $\delta^{18}O$ in ‰ (right panel) during the austral summer, i.e December to February (a,b) and winter, i.e. June to August(c,d) (for the Australian sector).

Figure 2: REMOiso simulations of mean precipitation in mm month^{-1} (left panel) and $\delta^{18}O$ in ‰ (right panel) during the austral summer, i.e December to February (a,b) and winter, i.e. June to August(c,d) (for the South American sector).

Figure 3: REMOiso simulations of mean precipitation in mm month^{-1} (left panel) and $\delta^{18}O$ in ‰ (right panel) during the boreal winter, i.e. December to February (a,b) and summer, i.e. June to August (c,d) (for the European sector)

Figure 4: Comparison of annual cycles for precipitation, surface air temperature and $\delta^{18}O$ at iPILPS sites. The left column displays forcing at Manaus, the middle column displays forcing at Neuherberg and the right column displays forcing at Tumbarumba. The upper row represents precipitation (in kg m^{-2} s^{-1}), the middle row represents $\delta^{18}O$ in precipitation (in ‰) and the bottom row represents temperature in the model's lowest atmospheric layer (in K). Grey solid lines represent REMOiso variable means, flanked as dashed lines by its 25%, 50% and 75% percentiles. The solid black lines for temperature and precipitation represent the GHCN data, while the dashed black lines represent the GNIP $\delta^{18}O$, precipitation and temperature observations. As Tumbarumba is not an GNIP station, we plotted the two nearest GNIP stations: Melbourne (dashed) and Adelaide (dash-dotted).

Figure 5: Comparison between REMOiso simulations and ABOM (Australian Bureau of Meteorology) data using monthly precipitation. The boxplots are constructed from

9 REMOiso grid cells closest to each station (i.e. n = 4 years x 9 cells for each boxplot). The dashed-open circle line shows the mean monthly rainfall from the observational ABOM 30+ year climatology.

Figure 6: Comparison between REMOiso and ABOM data using monthly temperature. The boxplots are constructed from 9 REMOiso grid cells closest to each station (i.e. n = 4 years x 9 cells for each boxplot). The dashed-open circle line shows the mean daily minmum and maximum monthly temperature from the observational ABOM 30+ year climatology. The mean monthly temperature from the ABOM is also shown (solid line).

Figure 7: Comparison between REMOiso and GNIP data using $\delta^{18}O$ in monthly precipitation. The boxplots are constructed from 9 REMOiso grid cells closest to each station (i.e. n = 4 years x 9 cells for each boxplot). The dashed-open circle line shows the mean monthly $\delta^{18}O$ from the observational GNIP data for each station..

Figure 8: Boxplots for meteorological variables for each hour over a diurnal cycle, for 30 days in January and July, over 4 years for Manaus (i.e. n = 4 years x 30 days for each boxplot), as simulated by REMOiso. Surf. Air Temp. = surface air temperature, Surf. Air Pres. = surface air pressure, Surf. U Wind = surface eastward wind, Surf. V Wind = surface northward wind, Down. SW = downward shortwave radiation, Down. LW = downward longwave radiation.

Figure 9: Boxplots for the two main water isotopes in rainfall and vapour for each hour over a diurnal cycle, for 30 days in January and July, over 4 years for Manaus (i.e. n = 4 years x 30 days for each boxplot) , as simulated by REMOiso. PREC =

precipitation, δPREC18 = $\delta^{18}O$ in precipitation, Qair = specific humidity, δQair18 = $\delta^{18}O$ in atmospheric water vapour.

Figure 10: Boxplots for meteorological variables for each hour over a diurnal cycle, for 30 days in January and July, over 4 years for Neuherberg (i.e. n = 4 years x 30 days for each boxplot), as simulated by REMOiso. Axis label abbreviations are the same as in Figure 8.

Figure 11: Boxplots for the two main water isotopes in rainfall and vapour for each hour over a diurnal cycle, for 30 days in January and July, over 4 years for Neuherberg (i.e. n = 4 years x 30 days for each boxplot) , as simulated by REMOiso. Axis label abbreviations are the same as in Figure 9.

Figure 12: Boxplots for meteorological variables for each hour over a diurnal cycle, for 30 days in January and July, over 4 years for Tumbarumba (i.e. n = 4 years x 30 days for each boxplot) , as simulated by REMOiso. Axis label abbreviations are the same as in Figure 8.

Figure 13: Boxplots for the two main water isotopes in rainfall and vapour for each hour over a diurnal cycle, for 30 days in January and July, over 4 years for Tumbarumba (i.e. n = 4 years x 30 days for each boxplot), as simulated by REMOiso. Axis label abbreviations are the same as in Figure 9.

Figures:

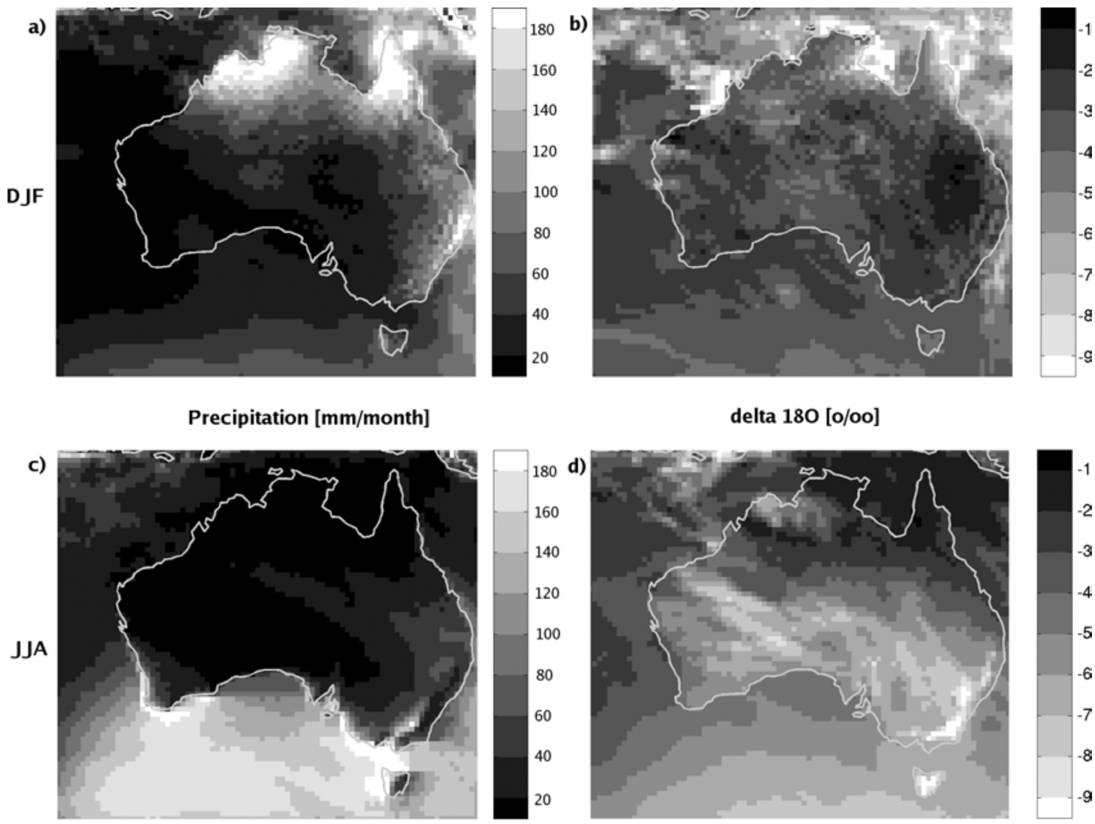

Figure 1

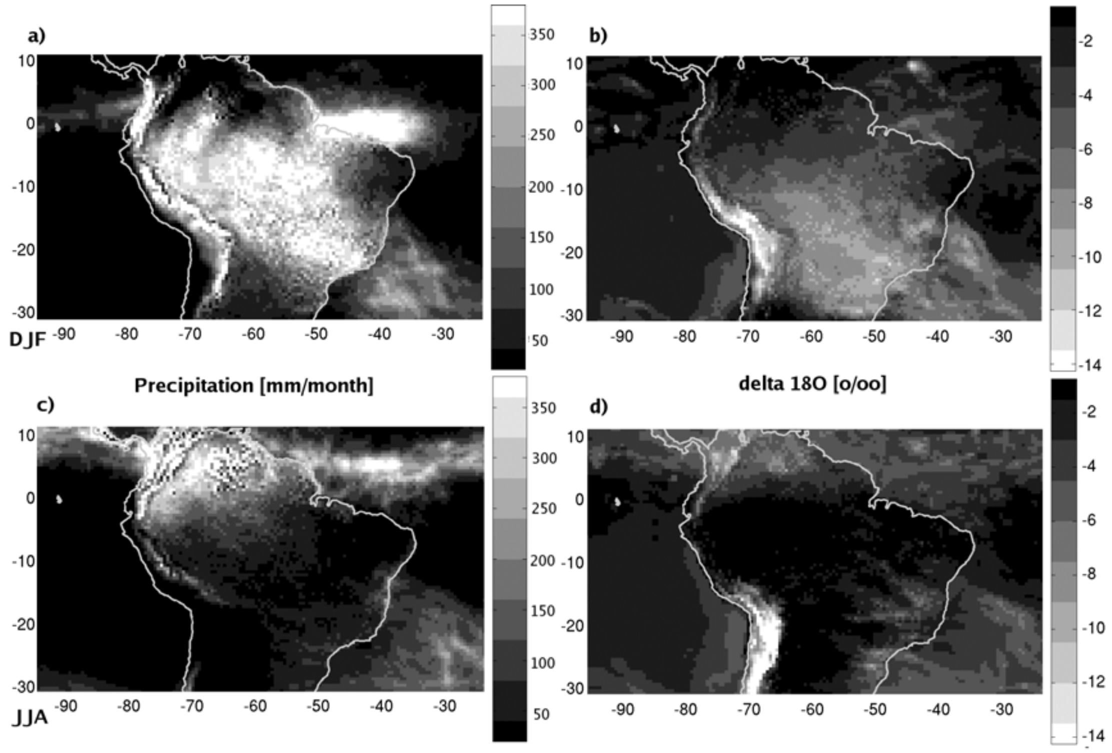
a)
b)
c)
d)
DJF
JJA
Precipitation [mm/month]
delta 18O [o/oo]
10
0
-10
-20
-30
-90
-80
-70
-60
-50
-40
-30
350
300
250
200
150
100
50
-2
-4
-6
-8
-10
-12
-14

Figure 2

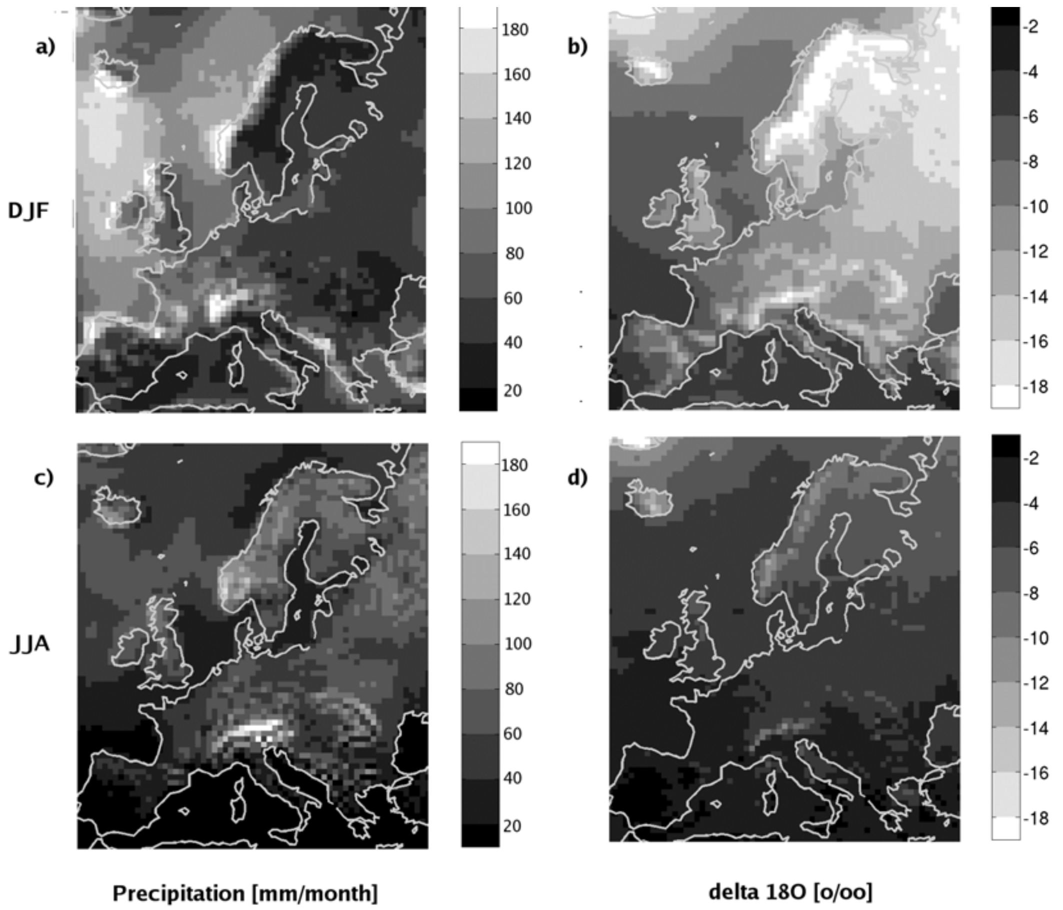
a)
b)
c)
d)
DJF
JJA
180
160
140
120
100
80
60
40
20
-2
-4
-6
-8
-10
-12
-14
-16
-18
Precipitation [mm/month]
delta 18O [o/oo]

Figure 3

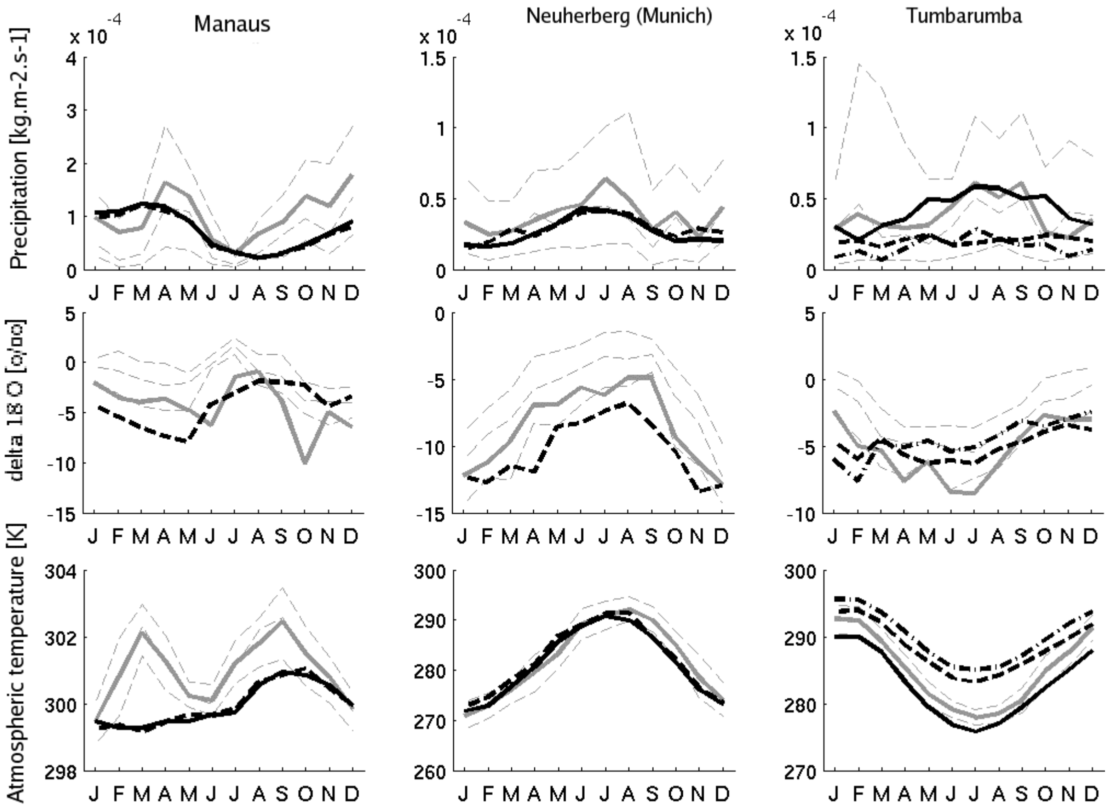
Manaus
Neuherberg (Munich)
Tumbarumba
Precipitation [kg.m-2.s-1]
delta 18 O [o/oo]
Atmospheric temperature [K]
x 10^-4
J F M A M J J A S O N D

Figure 4

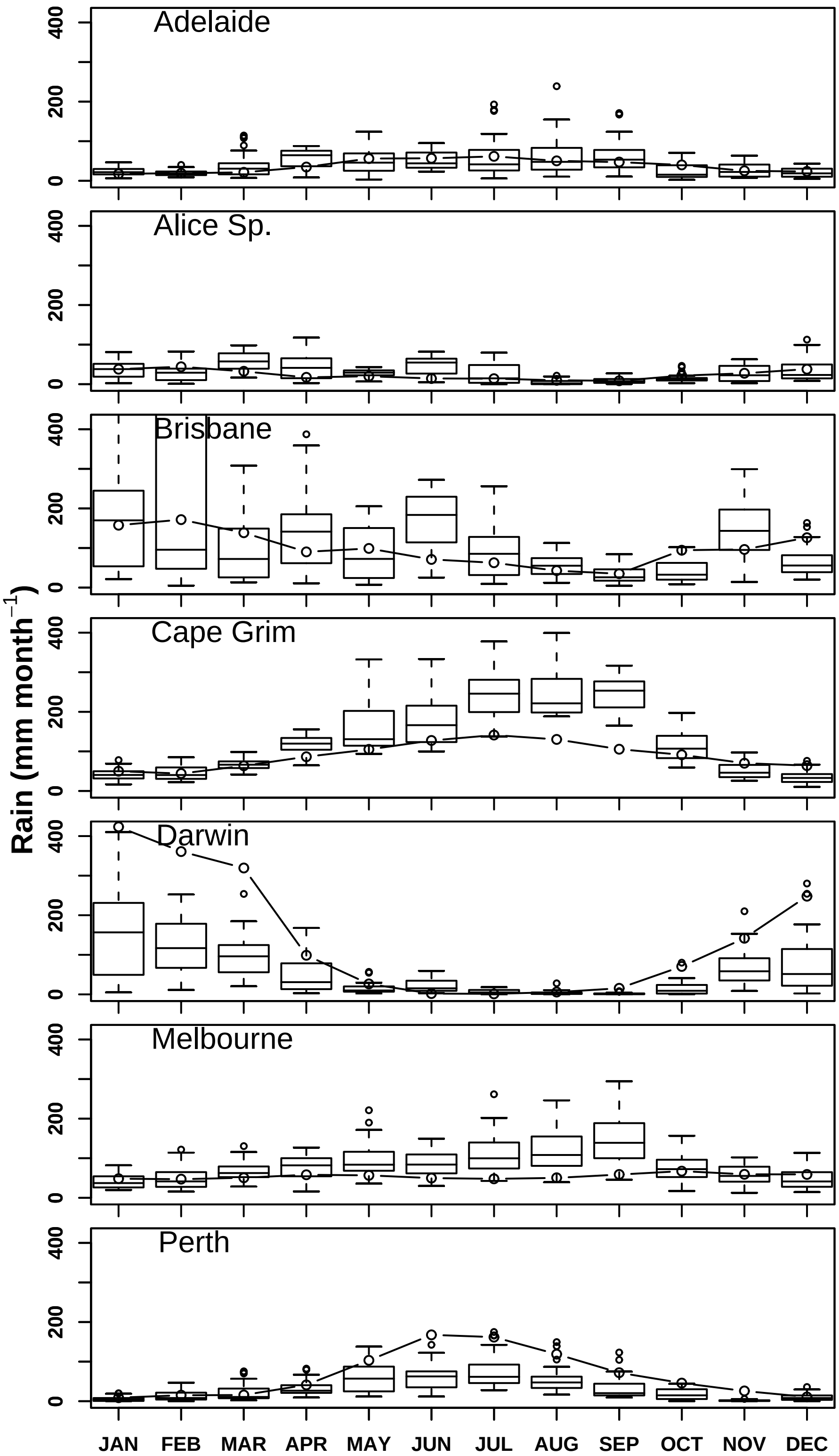

Adelaide
Alice Sp.
Brisbane
Cape Grim
Darwin
Melbourne
Perth
Rain (mm month⁻¹)
0
200
400
JAN
FEB
MAR
APR
MAY
JUN
JUL
AUG
SEP
OCT
NOV
DEC

Figure 5

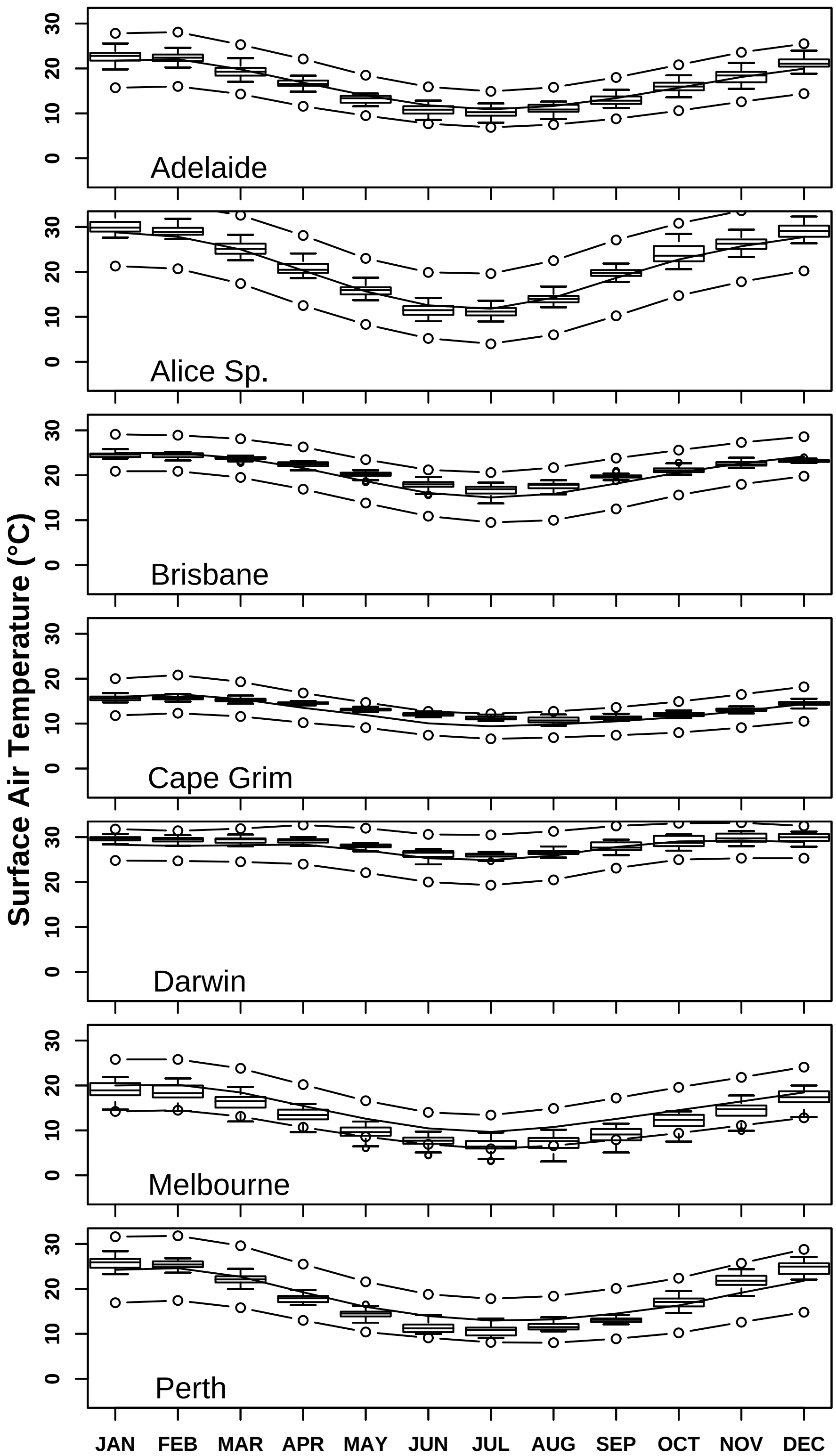
Surface Air Temperature (°C)
0
10
20
30
Adelaide
Alice Sp.
Brisbane
Cape Grim
Darwin
Melbourne
Perth
JAN
FEB
MAR
APR
MAY
JUN
JUL
AUG
SEP
OCT
NOV
DEC

Figure 6

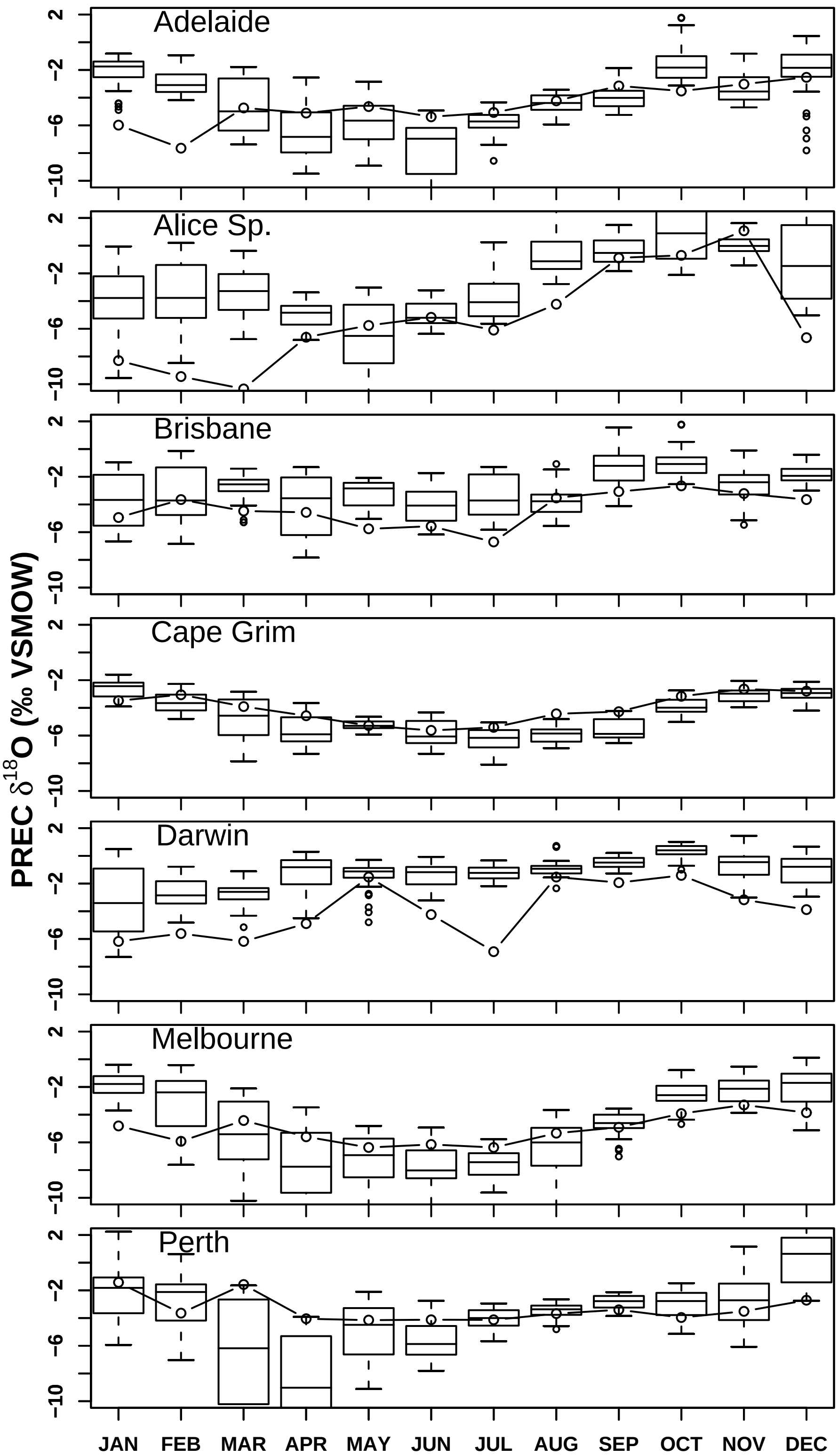
Adelaide
Alice Sp.
Brisbane
Cape Grim
Darwin
Melbourne
Perth
PREC δ18O (‰ VSMOW)
2
−2
−6
−10
JAN
FEB
MAR
APR
MAY
JUN
JUL
AUG
SEP
OCT
NOV
DEC

Figure 7

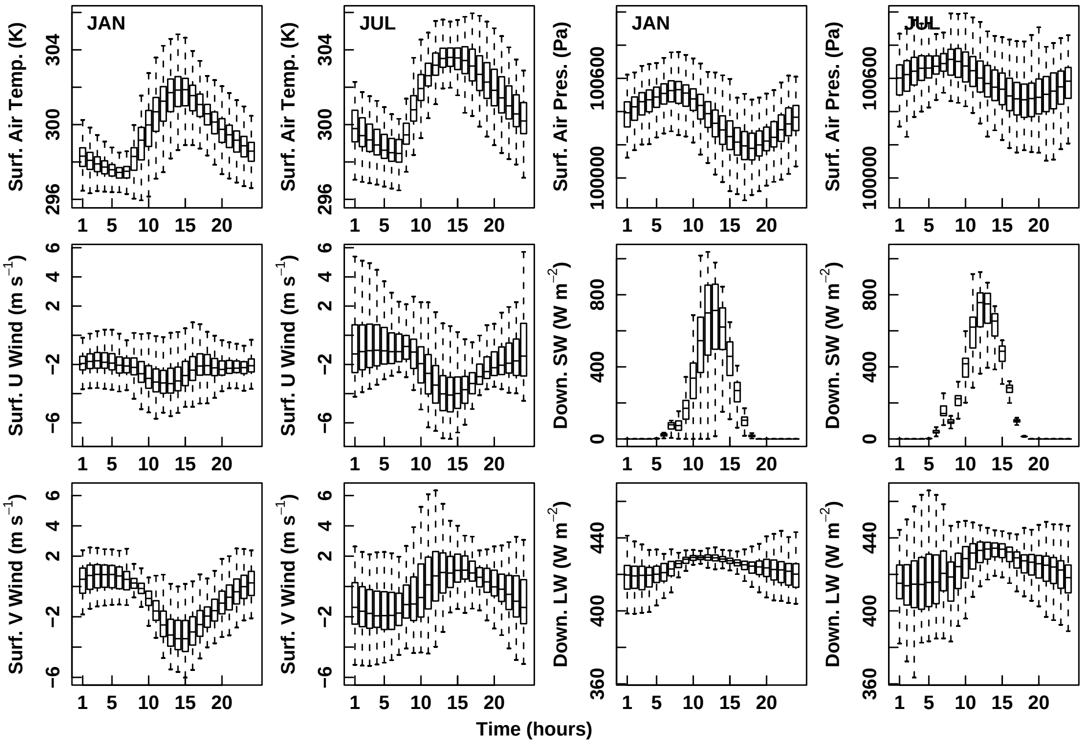

Figure 8

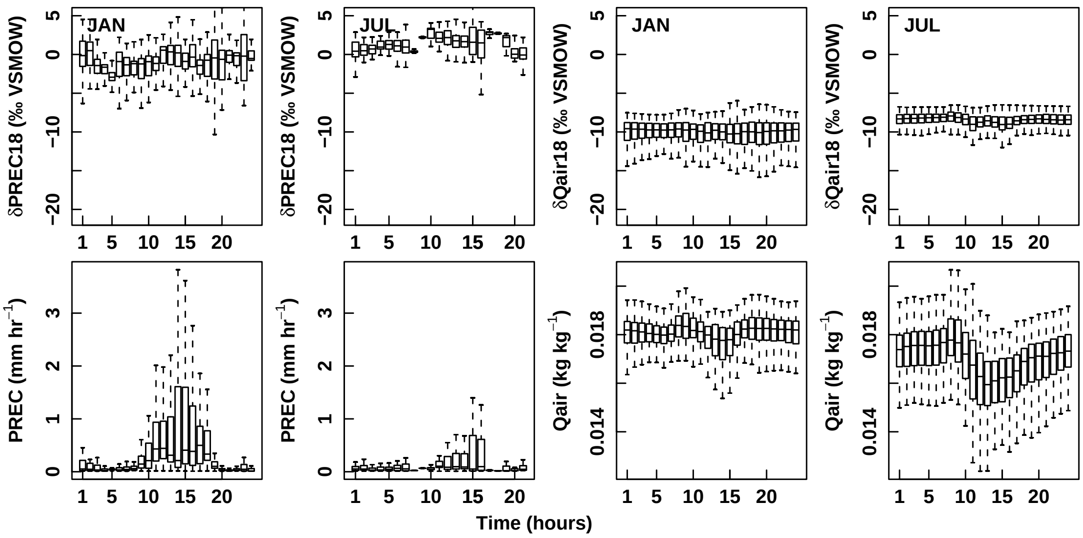

Figure 9

.

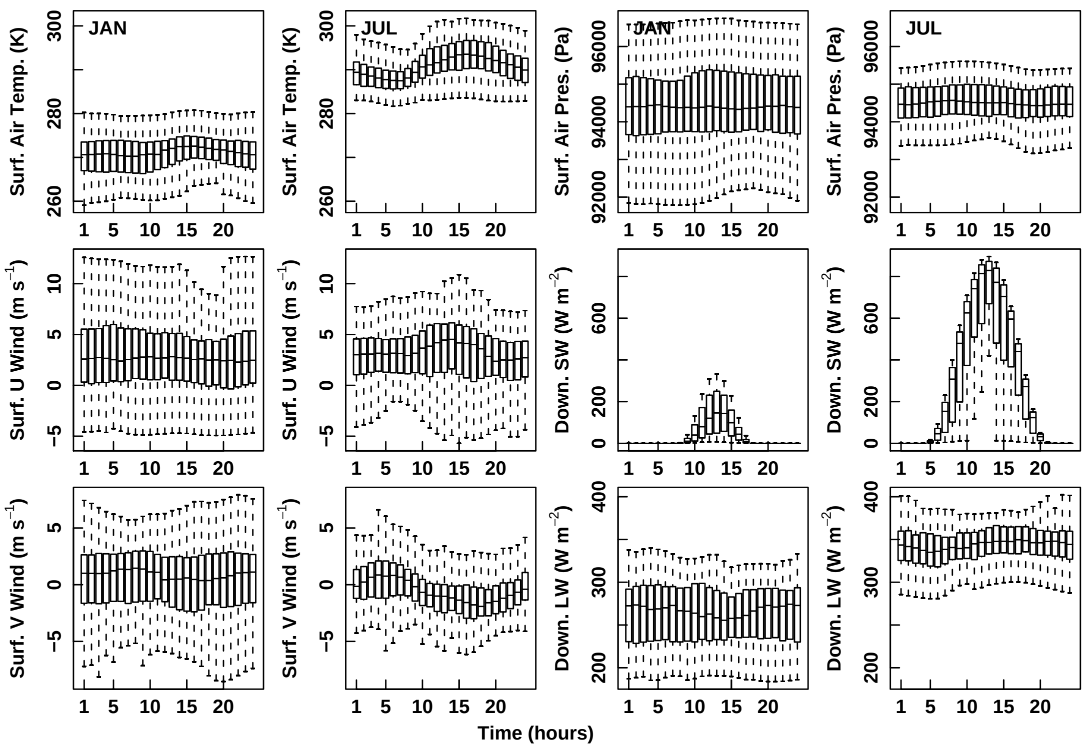

Figure 10

.

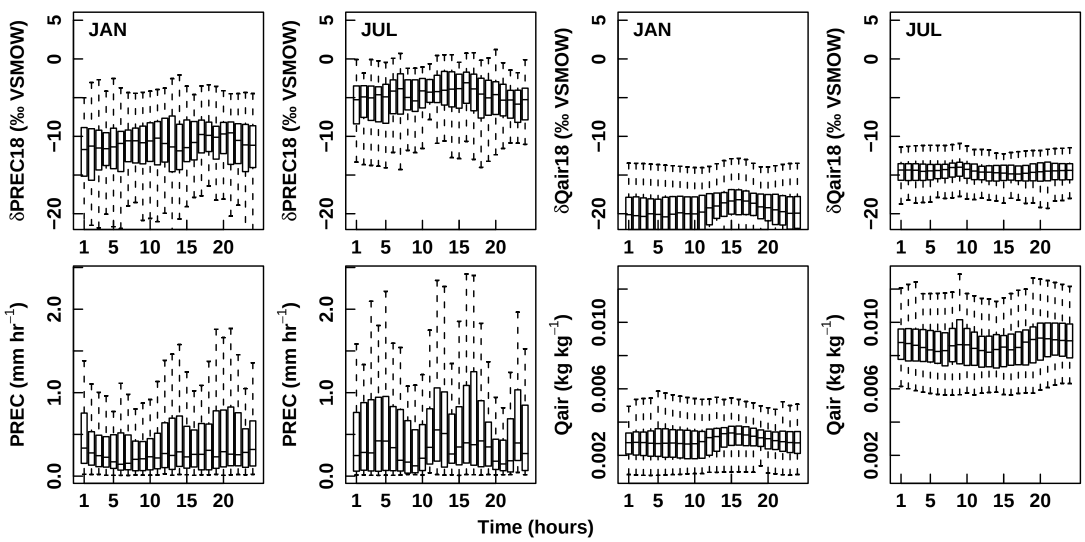

Figure 11

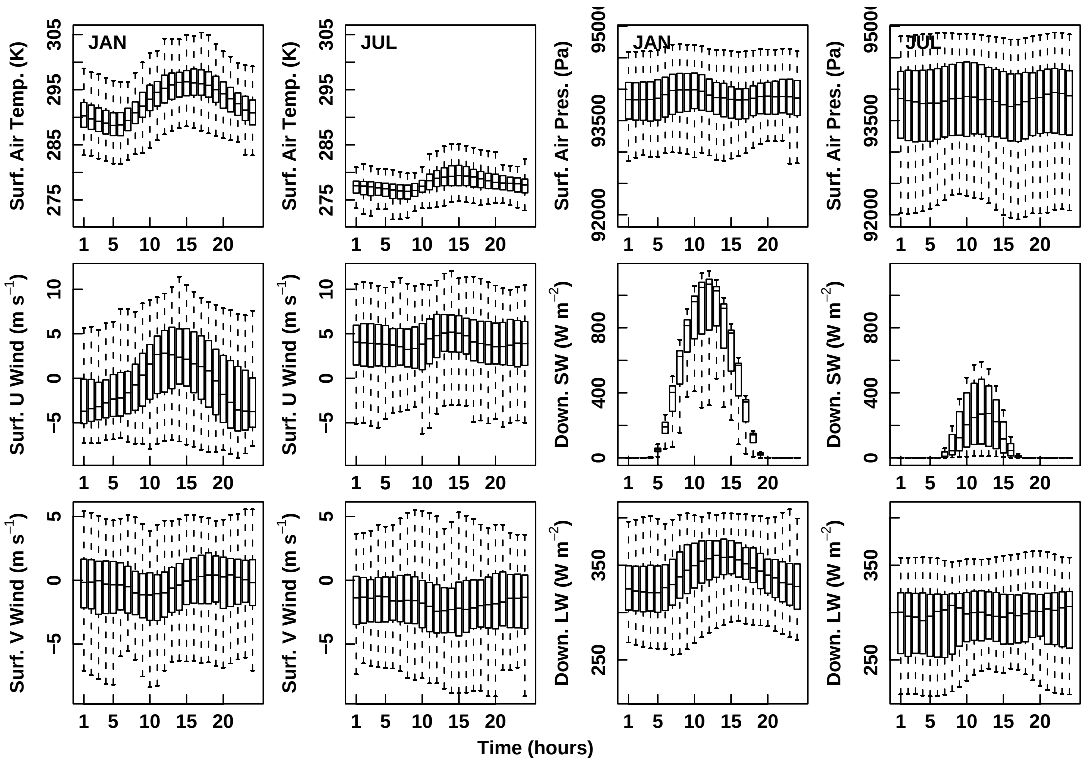

Figure 12

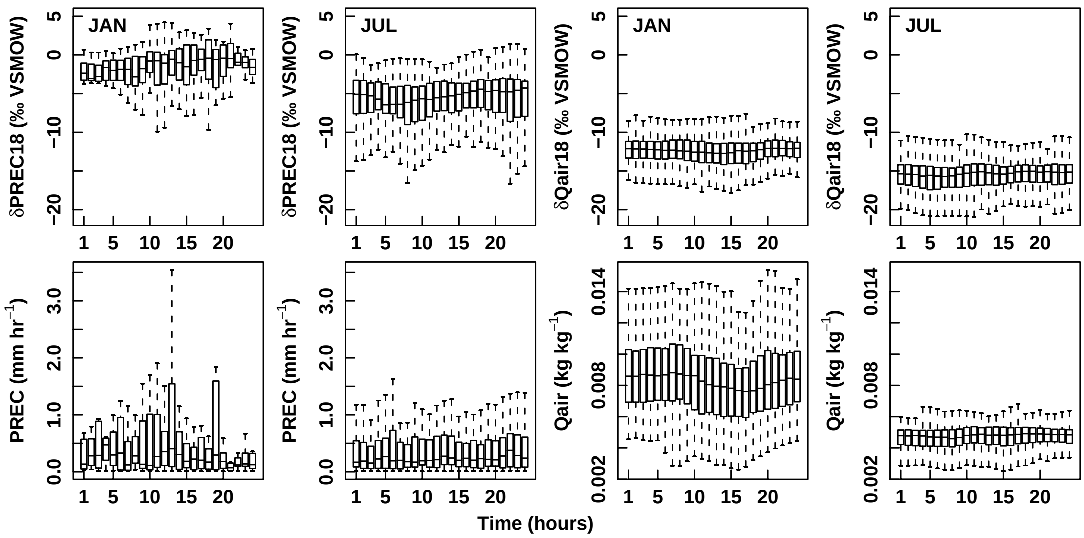

Figure 13